Supplementary Material

Table S1. Oligonucleotide primers used for cloning or real-time PCR

Name	Direction	Sequences (5' to 3')
hsa-miR-31-5p cloning primer	Sense	CTAGCAGCTATGCCAGCATCTTGCCUCCAGCTATGCCA GCATCTTGCC
	Antisense	AGCTGGCAAGATGCTGGCATAGCTGGAGGCAAGATGC TGGCATAGCTG
ACOX1 3' UTR - wild type reporter primer	Forward	AGGCCGGCCACTAGACTGCCACTGACAAG
	Reverse	AGGAGCTCTGCAGTAGCTCACTCCTGTAAT
ACOX1 3' UTR - mutagenic reporter primer	Forward	ACTCCAAACACTTGGAAGCTTAGAAAATCCATTGCA
hsa-miR-31-5p stem-looped RT primers		CTCAACTGGTGTCGTGGAGTCGGCAATTCAGTTGAGAG CTATGC
hsa-miR-31-5p	Forward	CGGCGGAGGCAAGATGCTGGCA
	Reverse	CAACTGGTGTCGTGGAGTCGG
U6	Forward	CTCGCTTCGGCAGCACA
	Reverse	AACGCTTCACGAATTTGCGT
ACOX1	Forward	CTGTAGGACCATTGTCTCG
	Reverse	TTACACTCTGCACTCCAAAG
ACAA2	Forward	TTGGCTGTTGAGAGGAGT
	Reverse	AATTCGTGAACCAGGTGT
ACADSB	Forward	GATTCTCATGCCTCATCCT
	Reverse	TATCCAGAAGCCAGAAGACC
HADH	Forward	AAAGAAGACATTGACACTGCTATGAAA
	Reverse	GCCACCCATCCACGATGA
MMP1	Forward	AACCTTTGATGCTATAACTACGAT
	Reverse	TTCAAGCCCATTTGGCAG
MMP2	Forward	TTGACCAGAATACCATCGAGAC
	Reverse	GGTGTGTAGCCAATGATCC
MMP3	Forward	AGAAGAGAAATTCCATGGAGC
	Reverse	CTCCAACTGTGAAGATCCAGTA
MMP9	Forward	CCTTTGGACACGCACGA
	Reverse	CAGGATGTCATAGGTCACGTA
MMP10	Forward	GATTTGATGAAAATAGCCAGTCC
	Reverse	CTGTGATGATCCACTGAAGAAGTA
EEF1A1	Forward	CAATGTGGGCTTCAATGTCAA
	Reverse	CATAGCCGGCGCTTATTTG

Table S2. 11 up-regulated miRNAs in oral cancer

miRNA name	Normal[1]	Tumor[1]	*p*-value	*q*-value	Fold change
hsa-miR-31-5p	13.10	16.00	6.71E-07	1.25E-06	7.42
hsa-miR-21-5p	12.66	14.93	3.64E-17	1.70E-15	4.84
hsa-miR-223-3p	14.02	15.80	1.49E-05	1.88E-05	3.45
hsa-miR-18a-5p	6.62	8.10	1.34E-08	4.18E-08	2.78
hsa-miR-21-3p	7.43	8.85	1.71E-07	3.80E-07	2.67
hsa-miR-135b-5p	7.95	9.28	9.38E-06	1.23E-05	2.52
hsa-miR-196b-5p	5.30	6.63	4.21E-03	2.36E-03	2.52
hsa-miR-491-5p	6.94	8.26	1.86E-05	2.12E-05	2.48
hsa-miR-223-5p	6.84	8.08	7.34E-04	5.11E-04	2.36
hsa-miR-34c-3p	5.22	6.39	6.62E-05	6.57E-05	2.25
hsa-miR-146b-5p	9.61	10.69	9.95E-03	4.69E-03	2.11

[1]Data are expressed as 40-Ct.

Table S3. KEGG pathway enrichment for putative targets of the six over-expressed miRNAs in OSCC

Term	Count	%	Fold Enrichment	*p*-value	Gene list
hsa00650:Butanoate metabolism	8	0.43	3.10	1.13E-02	ACSM2B, HMGCLL1, ALDH5A1, ACSM2A, HMGCS1, ECHS1, BDH2, HADH
hsa04962:Vasopressin-regulated water reabsorption	10	0.54	2.38	2.09E-02	RAB5B, DYNLL2, RAB5C, RAB5A, RAB11B, RAB11A, DCTN5, DCTN6, AQP3, NSF
hsa01212:Fatty acid metabolism	10	0.54	2.18	3.52E-02	ACAA2, ACOX1, ACADSB, PPT2, ECHS1, PPT1, HADH, ACSL3, ACSL6, ACOX3
hsa04520:Adherens junction	13	0.70	1.92	3.48E-02	CDC42, PARD3, WASF3, RAC2, ACTN4, TGFBR2, RAC1, MET, SMAD2, PTPN1, SRC, CTNNA3, VCL
hsa04146:Peroxisome	14	0.75	1.77	4.95E-02	ECI2, ACOX1, HMGCLL1, PEX5, ACOX3, PEX2, GSTK1, PEX26, HAO2, PXMP4, ABCD3, HSD17B4, ACSL3, ACSL6
hsa04110:Cell cycle	20	1.07	1.69	2.52E-02	CDC7, CDK1, SKP2, CDC23, SMAD2, ANAPC10, SKP1, MCM2, YWHAE, SMC3, WEE1, CDK2, ATM, RBX1, HDAC2, CCND2, ORC4, TFDP2, STAG2, SMC1B
hsa04910:Insulin signaling pathway	22	1.18	1.67	2.06E-02	IRS4, FLOT1, FBP1, RHOQ, MAPK10, FBP2, PPP1R3A, RPS6, PPP1CC, IRS1, G6PC3, PPP1R3D, NRAS, PRKAR2A, PPP1R3B, SLC2A4, CALM3, MAPK8, PTPN1, SHC3, AKT3, CALM1
hsa05168:Herpes simplex infection	29	1.56	1.66	7.78E-03	SRSF1, FASLG, HCFC2, TBP, OAS1, OAS2, IFNA2, IFNA1, TAP1, PER2, HLA-DPB1, TRAF5, TBPL1, CDK1, SP100, HLA-A, SKP2, MAPK10, SKP1, NXF1, PPP1CC, HLA-DQA2, CDK2, SRSF3, DDX58, SRSF2, IFNAR2, IL12A, MAPK8
hsa04722:Neurotrophin signaling pathway	19	1.02	1.66	3.48E-02	NTF3, FASLG, MAPK10, MAPKAPK2, YWHAE, IRS1, RPS6KA5, CDC42, NRAS, MAP3K1, RAC1, CAMK2D, CALM3, SORT1, MAPK8, SHC3, FRS2, AKT3, CALM1
hsa04068:FoxO signaling pathway	21	1.13	1.64	2.84E-02	IRS4, SGK3, ATG12, TGFBR2, SKP2, IGF1, BNIP3, FASLG, SMAD2, MAPK10, C8ORF44-SGK3, HOMER1, IRS1, G6PC3, CDK2, ATM, NRAS, SLC2A4, CCND2, MAPK8, AKT3
hsa04014:Ras signaling pathway	35	1.88	1.62	4.68E-03	FGF18, FGF7, RAB5B, RAB5C, FGF14, KITLG, FASLG, FGF10, ARF6, CDC42, RAC2, GRIN2B, TIAM1, RASGRP1, RAC1, PLA2G1B, PDGFC, GNG2, FGF1, SHC3, RASA1, AKT3, GNG7, PLA2G16, MET, IGF1, MAPK10, LAT, NRAS, VEGFC, RAB5A, CALM3, MAPK8, CALM1, PLA2G2F
hsa05202:Transcriptional misregulation in cancer	26	1.40	1.62	1.61E-02	CCNT1, PAX5, MMP3, MEIS1, WT1, ELK4, FCGR1A, ETV6, RUNX1, CDK14, MLLT3, ERG, TGFBR2, MET, IGF1, SPINT1, ATM, HDAC2, NUPR1, SP1, CCND2, BMP2K, HIST1H3B, H3F3C, HIST1H3H, KLF3
hsa05152:Tuberculosis	26	1.40	1.54	2.89E-02	RAB5B, RAB5C, PPP3R2, NFYB, TLR4, SRC, IFNA2, IFNA1, IL10RB, FCGR1A, PIK3C3, CAMK2D, HLA-DPB1, AKT3, BCL10, MALT1, MAPK10, HLA-DQA2, TRADD, CD209, RAB5A, IL12A, CALM3, MAPK8, CLEC7A, CALM1

Table S4. Enrichment of miR-31-5p predicted targets in KEGG pathways

Term	Count	%	Fold Enrichment	*p*-value	Gene list
hsa00071: Fatty acid metabolism	7	0.61	2.70	4.12E-02	ACAA2, ACOX1, ACADSB, ACSL4, HADH, ACADL, ACSL5
hsa04520: Adherens junction	13	1.12	2.61	3.47E-03	PTPRB, TCF7, BAIAP2, MET, SMAD2, SRC, ACVR1C, CDC42, PVRL4, RAC2, RAC1, PVRL2, PTPN1
hsa04310: Wnt signaling pathway	23	1.99	2.35	2.30E-04	TCF7, ROCK2, CAMK2G, PPP2R5C, FZD1, PPP3R2, SMAD2, FZD3, FZD4, PRKCB, WNT1, RAC2, CSNK1E, RAC1, CACYBP, NFAT5, FRAT1, CAMK2D, NFATC4, PPP3CA, PLCB1, AXIN1, APC
hsa04916: Melanogenesis	14	1.21	2.19	1.05E-02	TCF7, GNAI3, CAMK2G, MITF, ADCY6, FZD1, KITLG, FZD3, FZD4, PRKCB, EDNRB, WNT1, CAMK2D, PLCB1
hsa05416: Viral myocarditis	10	0.86	2.18	3.74E-02	CD55, RAC2, DMD, RAC1, HLA-A, MYH14, MYH6, MYH9, ABL2, CD28
hsa04012: ErbB signaling pathway	12	1.04	2.13	2.31E-02	NCK2, NRG3, ERBB4, CAMK2G, GAB1, MAP2K4, CAMK2D, CRK, ABL2, SRC, PRKCB, SHC4
hsa05210: Colorectal cancer	11	0.95	2.02	4.25E-02	TCF7, RAC2, MET, RAC1, FZD1, FZD3, SMAD2, FZD4, ACVR1C, AXIN1, APC
hsa04144: Endocytosis	23	1.99	1.93	3.36E-03	FAM125B, RET, FGFR3, ERBB4, RAB5B, RAB5C, MET, PSD3, HLA-A, ASAP2, RUFY1, PIP5K1A, SRC, ACVR1C, CDC42, RAB31, AP2B1, TFRC, ACAP3, NEDD4, ACAP2, NEDD4L, IQSEC2
hsa04360: Axon guidance	16	1.38	1.92	1.82E-02	ABLIM1, GNAI3, ROCK2, MET, PPP3R2, CXCL12, CDC42, NCK2, RAC2, SEMA6D, RAC1, NFAT5, SRGAP3, NFATC4, PPP3CA, RASA1

Figure S1

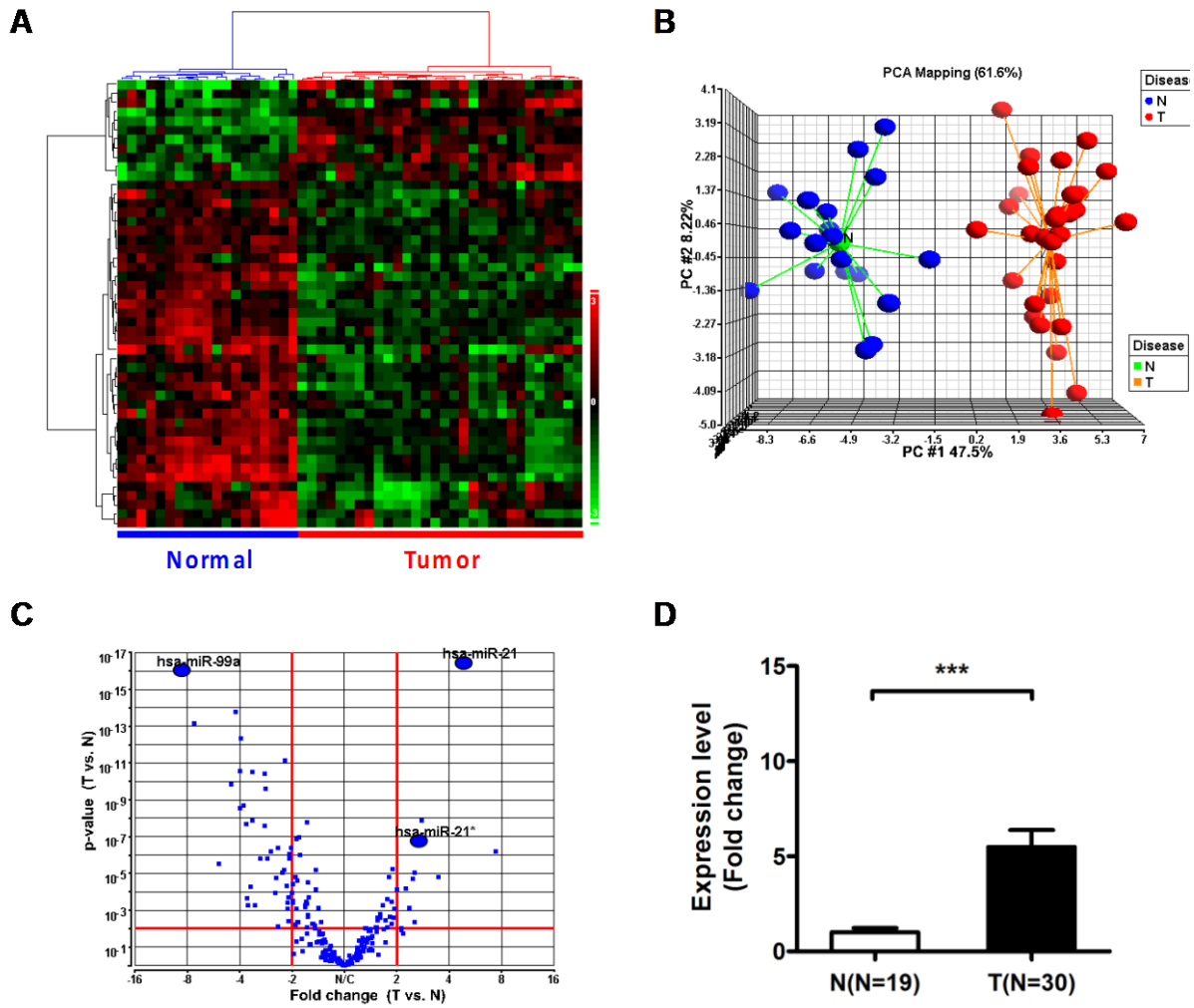

Figure S1. miR-31-5p is highly up-regulated in OSCC tissues.

Our patient cohort for the miRNA expression profiling experiment comprises specimens from 19 normal oral tissues and 30 tumor oral tissues. (A) Hierarchical clustering of the normal (blue) and tumor oral tissues (red) based on the expression levels of the 49 differentially expressed miRNAs. (B) Principal component analysis (PCA) of the normal (blue) and OSCC samples (red) based on the expression of 232 miRNAs. (C) Volcano plot of fold change and probability values (*p*-values) for all individual miRNAs in OSCC compared with normal samples. (D) The expression levels of miR-31-5p in OSCC are expressed relative to the normal control. ***, $p < 0.001$, Student's t-test.

Figure S2

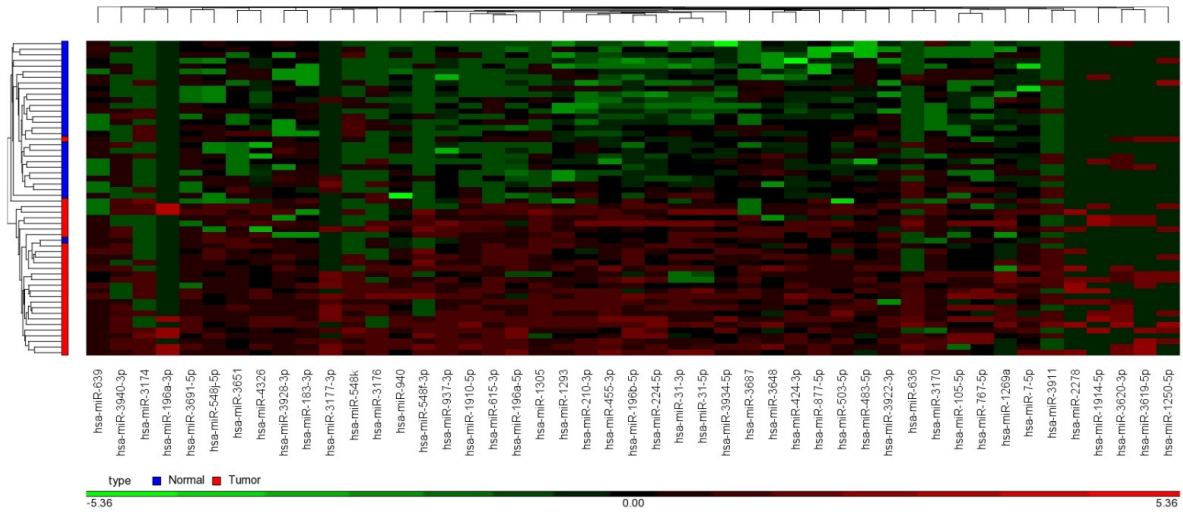

Figure S2. miR-31-5p is over-expressed in OSCC tissues.

Hierarchical clustering of 28 normal/tumor paired OSCC samples based on the expression levels of 47 significantly up-regulated miRNAs.

Figure S3

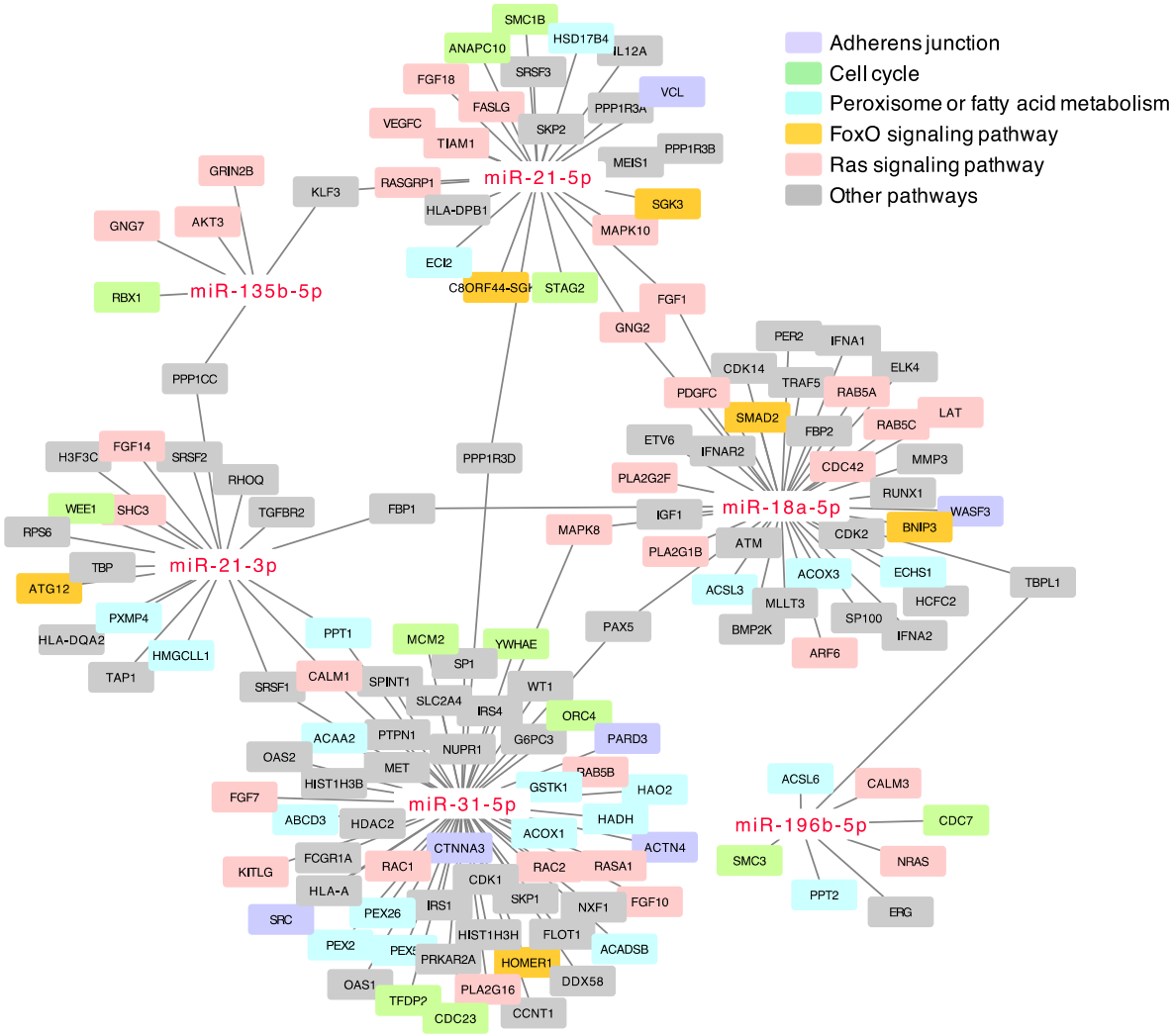

Figure S3. miRNA-mRNA interactome network of the six up-regulated miRNAs in OSCC.

For the six up-regulated mRNAs in OSCC identified by this study, miRNA-mRNA interactions were constructed by computational target prediction. All miRNAs are highlighted in red in the center of sub-networks, while putative target genes are displayed with different colored nodes based on the indicated functional annotation pathways.

Figure S4

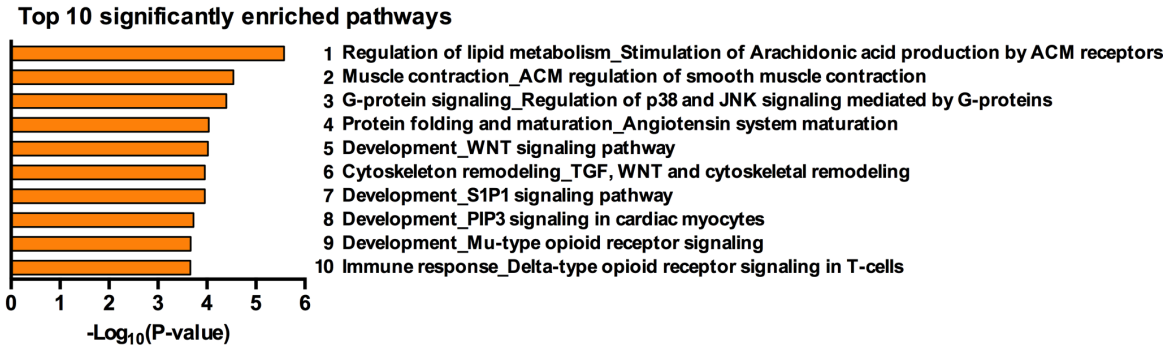

Figure S4. The putative miR-31-5p targets are enriched in the regulation of lipid metabolism pathway.

GeneGo MetaCore gene enrichment analysis of predicted miR-31-5p targets. The top 10 significantly enriched pathways are shown.

Figure S5

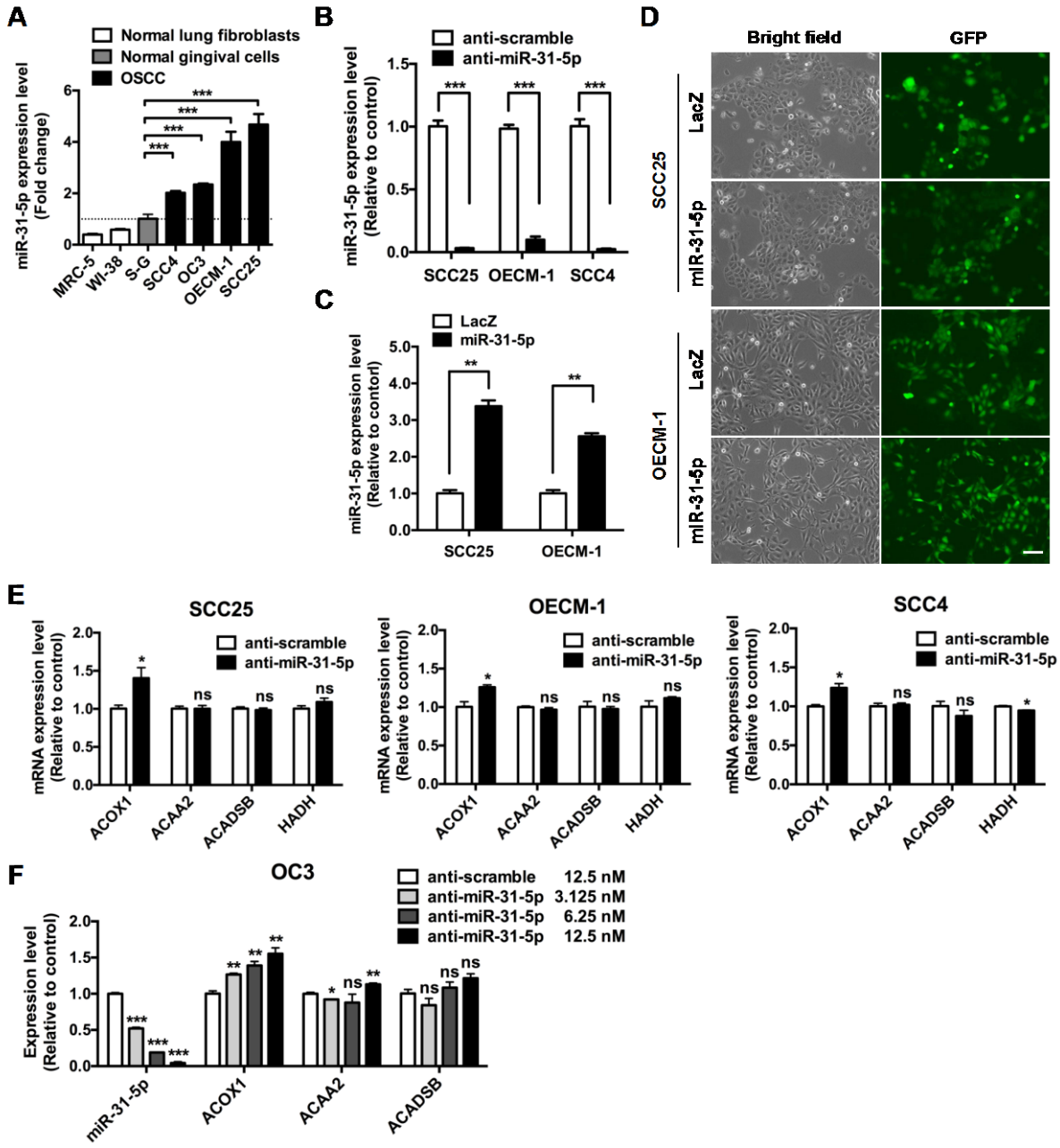

Figure S5. Identification of miR-31-5p targets in the lipid metabolism pathway.

(A) Relative expression levels of miR-31-5p in two normal lung fibroblast cell lines (MRC-5 and WI-38), a normal gingival cell line (S-G) and four OSCC cells lines, were determined using stem loop qRT-PCR and expressed as fold changes relative to the S-G cell line. (B) to (D) Establishment of miR-31-5p LNA-based knockdown and lentiviral-based over-expression systems in OSCC lines. (B) Expression levels of miR-31-5p in SCC25, OECM-1 and SCC4 cells transfected with miR-31-5p antisense oligomers (anti-miR-31-5p) or scramble control (anti-scramble). (C-D) Expression

levels of miR-31-5p in SCC25 and OECM-1 cells lentivirally infected with miR-31-5p over-expression or control (LacZ) vector (C). The infection efficiency was evaluated by GFP co-expression (D). Scale bar, 100 μm. miR-31-5p expression levels were determined via stem loop qRT-PCR. (E) Expression levels of ACOX1, ACAA2, ACADSB and HADH in miR-31-5p-knockdown SCC25, OECM-1 and SCC4 cells were measured by qRT-PCR and expressed as fold change relative to control. (F) Expression levels of miR-31-5p, ACOX1, ACAA2 and ACADSB in OC3 transfected with indicated doses of miR-31-5p antisense oligomers (anti-miR-31-5p) or scramble control (anti-scramble) for 48 hrs. All data are shown as mean ± SEM from three independent experiments (ns, not significant; *, $p < 0.05$; **, $p < 0.01$; ***, $p < 0.001$; Student's t-test).

Figure S6

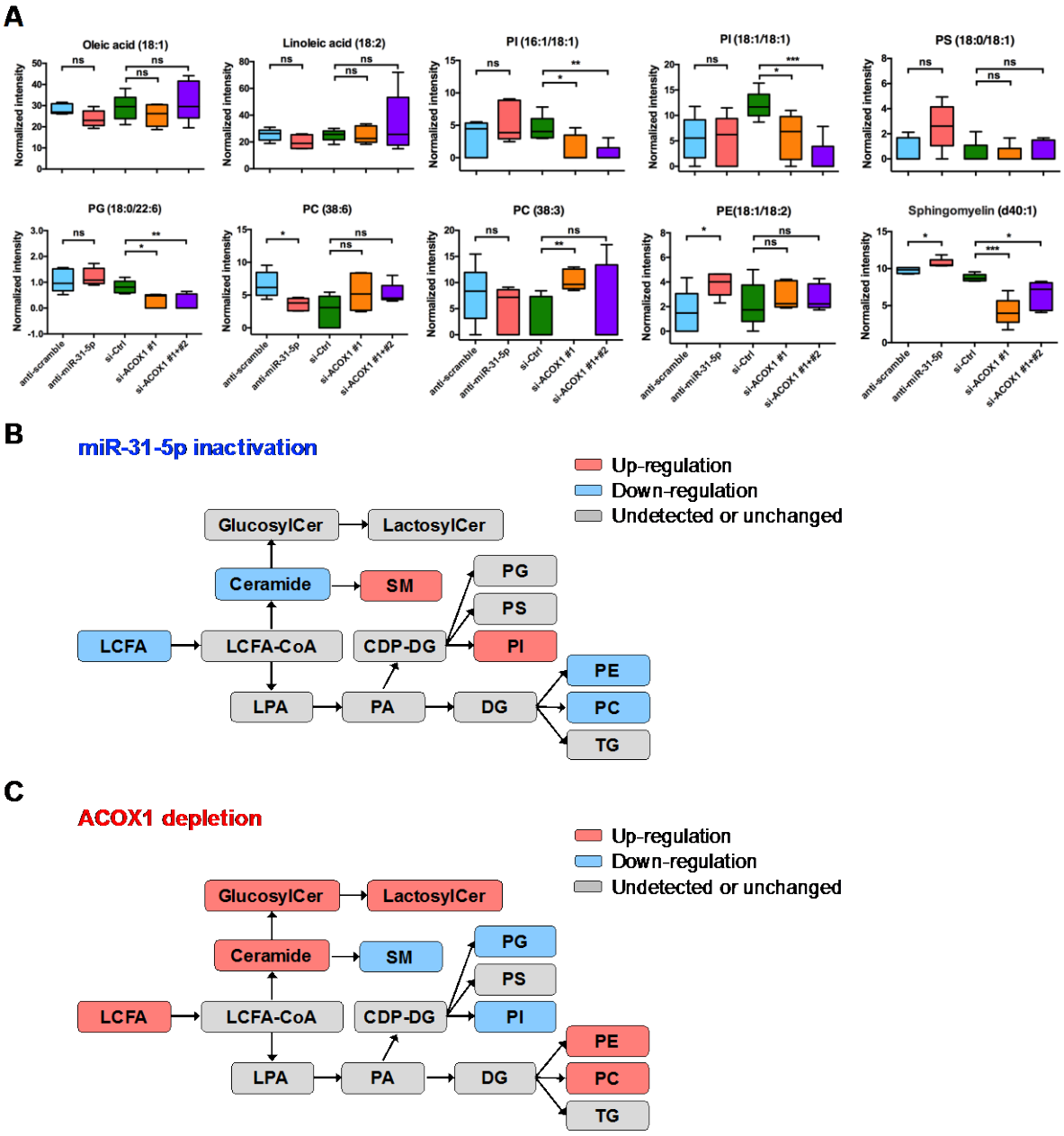

Figure S6. miR-31-5p and ACOX1 alter the lipidomic profiles of OSCC cells in an antagonistic manner.

(A) Intensity of the indicated lipid metabolites was determined using UPLC-MS, and the data are shown as mean ± SEM from at least three independent repeats. (B-C) Schematic diagram of the altered lipid metabolic pathways in SCC25 cells upon miR-31-5p inactivation (B) or ACOX1 depletion (C). The up- and down-regulated lipid metabolites are marked with red and blue color, respectively, while the undetected or

unchanged metabolites are depicted in gray. LCFA: long chain fatty acid; LPA: lysophosphatidic acid; PA: phosphatidic acid; CDP-DG: cytidine diphosphate diacylglycerol; DG: diacylglycerol; PE: phosphatidylethanolamine; PC: phosphatidylcholine; TG: triacylglycerol; PG: phosphatidylglycerol; PS: phosphatidylserine; PI: phosphatidylinositol; GlucosylCer: glucosylceramide; LactosylCer: lactosylceramide; SM: sphingomyelin.

Figure S7

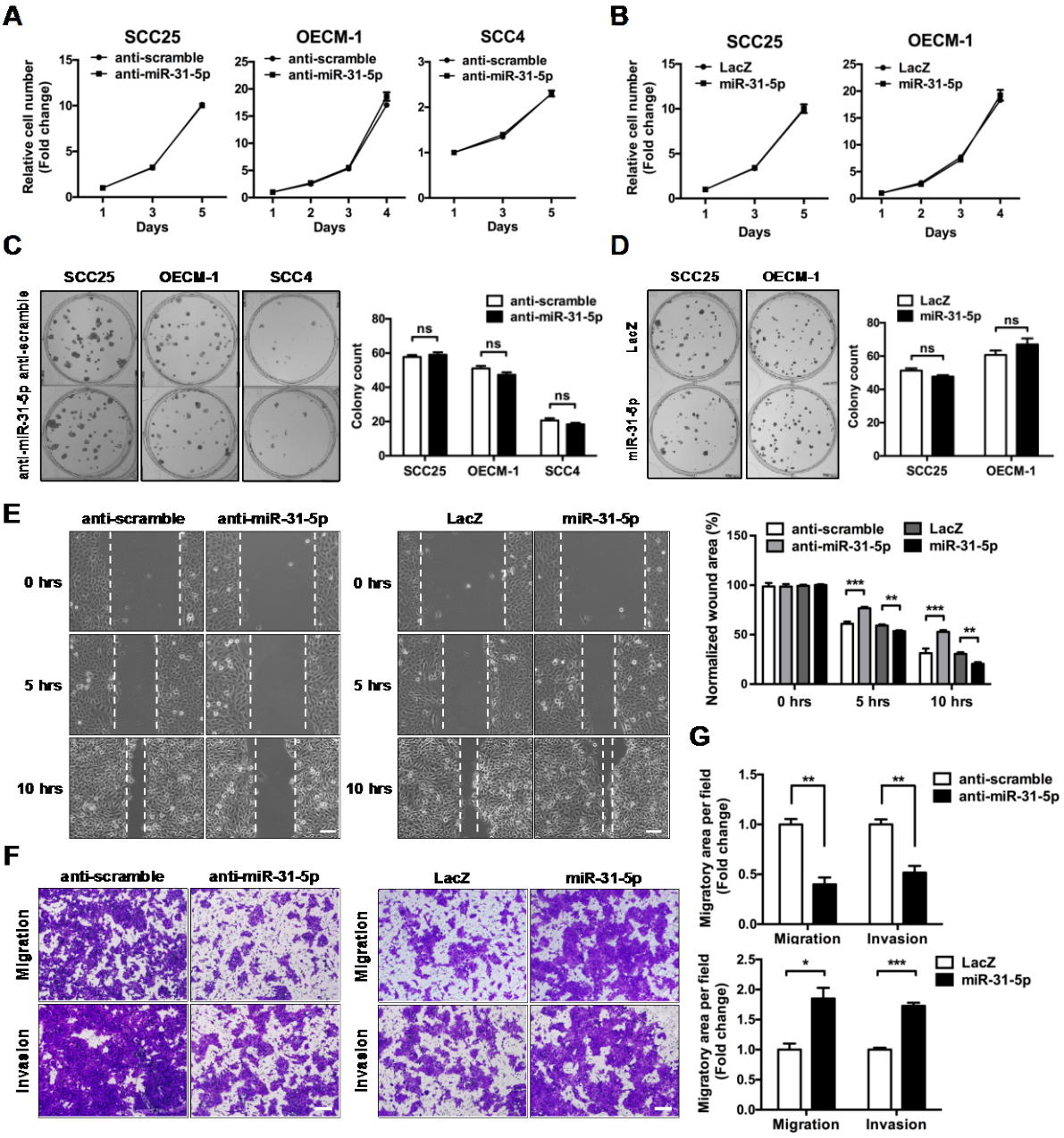

Figure S7. miR-31-5p promotes the migration and invasiveness of OSCC cells irrespectively of cell proliferation.

(A-B) Growth curve analysis was performed on SCC25, OECM-1 and SCC4 cells transfected with LNA-modified miR-31-5p antisense oligomers (anti-miR-31-5p) or scramble control (anti-scramble) (A) or on SCC25 and OECM-1 cells infected with lentiviruses carrying the miR-31-5p or control (LacZ) vector (B). Data were normalized to Day1 and expressed as mean ± SEM. (C-D) Colony forming activity of miR-31-5p knockdown SCC25, OECM-1 and SCC4 cells (C) and miR-31-5p over-expressing

cells (D), as indicated. Representative images of crystal violet staining are shown on the left, while quantitative results of three independent experiments are shown on the right. (E-G) OECM-1 cells were subjected to miR-31-5p knockdown or over-expression, and analyzed by wound healing migration assay (E) and transwell migration and Matrigel invasion assays (F-G). Data are shown as mean ± SEM from three independent experiments (*, $p < 0.05$; **, $p < 0.01$; ***, $p < 0.001$; Student's t-test).

Figure S8

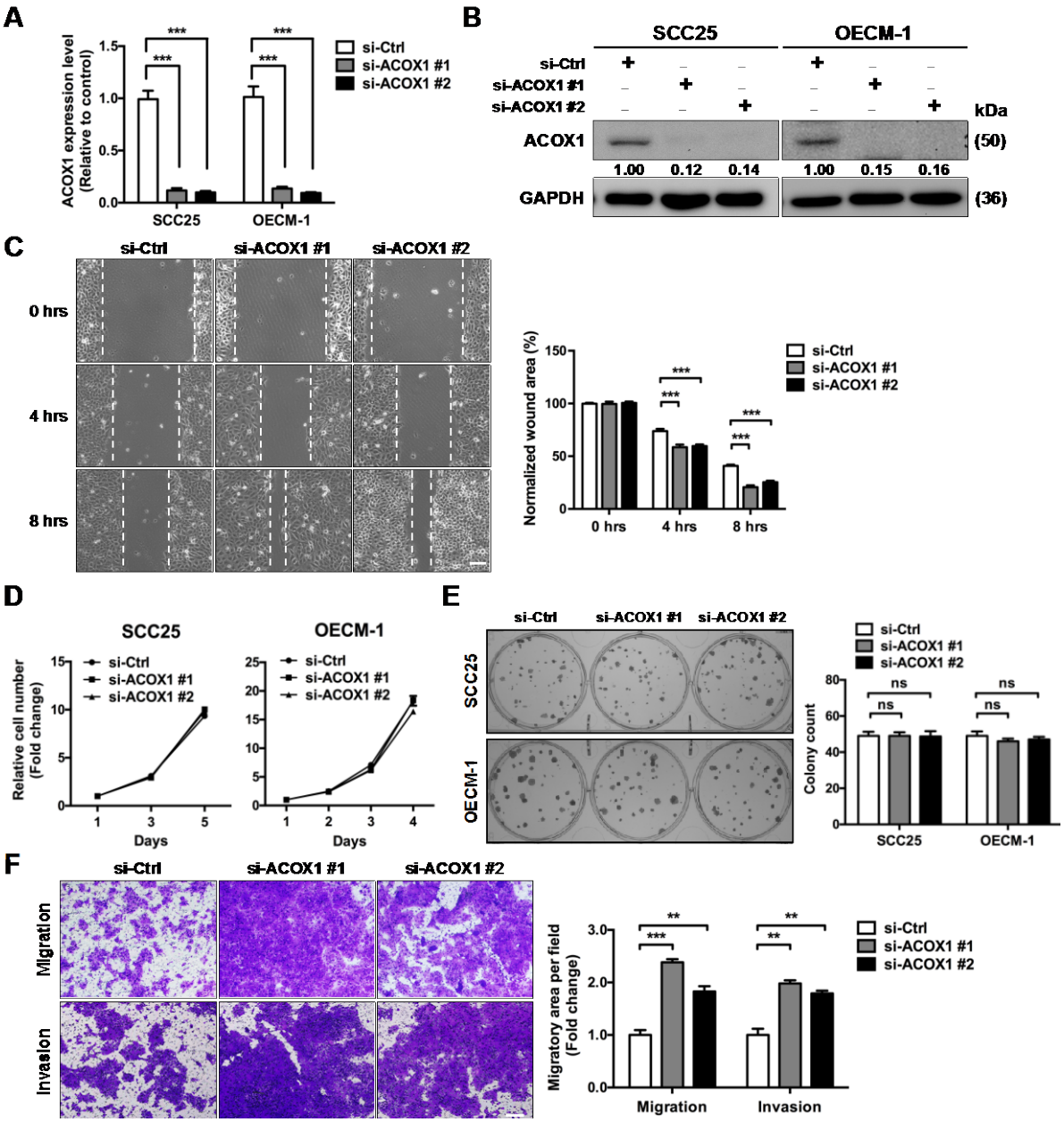

Figure S8. Knockdown of ACOX1 promotes OSCC cell migration and invasion. (A) Expression levels of ACOX1 in SCC25 and OECM-1 cells transfected with two different ACOX1 siRNAs (si-ACOX1 #1 or si-ACOX1 #2) or siRNA-negative control (si-Ctrl). Data are expressed as mean ± SEM from three independent experiments (***, $p < 0.001$). (B) Protein levels of ACOX1 in cells shown in (A) were determined by western blotting, with GAPDH as the loading control. (C) *In vitro* migratory abilities of OECM-1 cells upon ACOX1 depletion were measured. (D) Growth curve analysis was performed on SCC25 and OECM-1 cells treated with ACOX1 siRNAs or control. Data were normalized to Day1 and expressed as mean ± SEM. (E) Colony forming activity

was determined for SCC25 and OECM-1 cells with ACOX1 knockdown. The representative images are shown (left panel); quantitative results, based on colony numbers, are also shown as mean ± SEM of three independent experiments (right panel) (ns, not significant). (F) Transwell invasion assay was performed on OECM-1 cells transfected with ACOX1 siRNAs (si-ACOX1 #1 or si-ACOX1 #2) or siRNA-negative control (si-Ctrl). Bar graphs in (C) and (F) depict mean ± SEM from three independent experiments (**, $p < 0.01$; ***, $p < 0.001$).

Figure S9

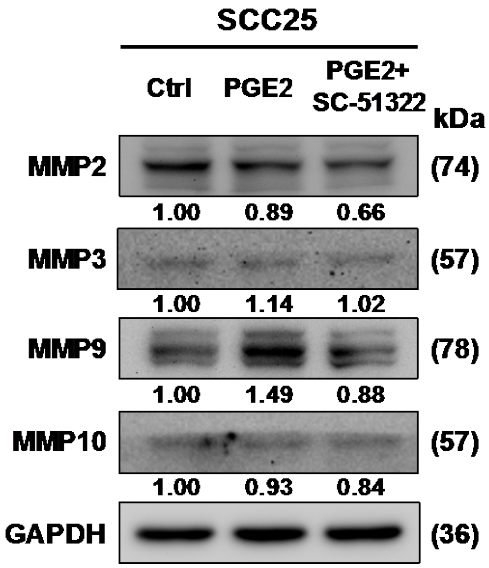

Figure S9. PGE2 triggers MMP9 protein up-regulation in SCC25 cells.

Protein levels of MMP2, MMP3, MMP9 and MMP10 in SCC25 cells, treated with control or 0.01 μM PGE2 alone or together with SC-51322, were determined by western blotting. GAPDH was used as a loading control. Abundance fold changes were quantified based on signal intensity and expressed relative to the control group.

Figure S10

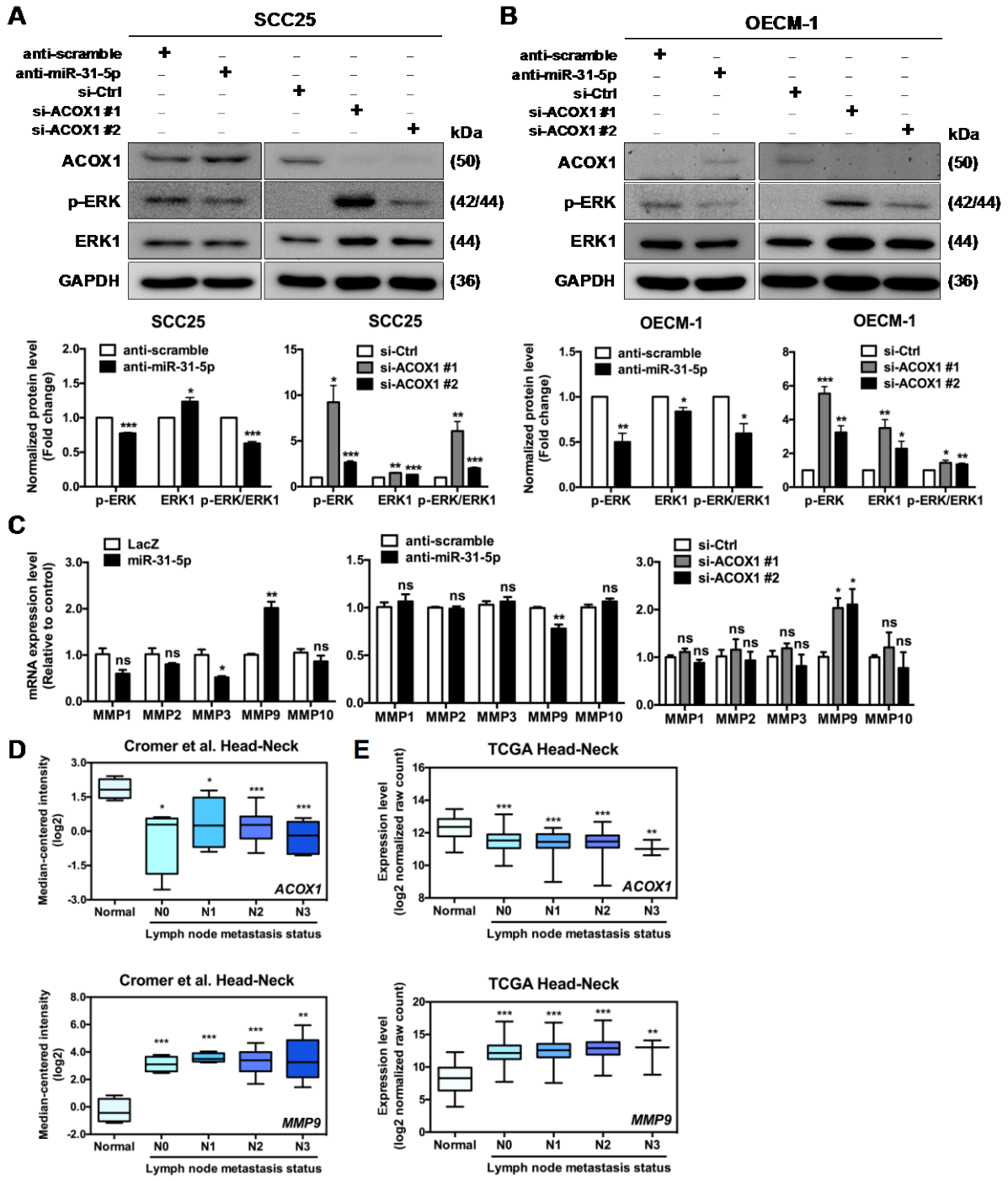

Figure S10. Link of miR-31-5p-ACOX1 axis to ERK-MM9 signaling in OSCC cells and clinical samples.

Inactivation of miR-31-5p or down-regulation of ACOX1 alters the ERK-MMP9 signaling in OSCC cells. (A-B) Western blot analysis of the indicated proteins in SCC25 (A) and OECM-1 (B) cells with miR-31-5p or ACOX1 knockdown. GAPDH was used as a loading control. (C) Expression levels of mRNAs encoding matrix

metalloproteinases MMP1, MMP2, MMP3, MMP9 and MMP10 in SCC25 cells were determined using qRT-PCR. RNAs were extracted from miR-31-5p over-expressing (left panel), miR-31-5p-depleted (middle panel) or ACOX1-depleted (right panel) cells. ACOX1 expression is inversely correlated with MMP9 level and with lymph node metastasis in HNSCC tissues. (D-E) Expression levels of ACOX1 (upper panel) and MMP9 (lower panel) were analyzed in normal and HNSCC samples sub-grouped according to lymph node metastasis status. Microarray data (Normal, n = 4; N0, n = 4; N1, n = 4; N2, n = 20; N3, n = 6) from Oncomine online database (GEO accession number: GSE2379) were processed and presented as log2 median-centered intensity (D). RNA sequencing dataset (Normal, n = 43; N0, n = 109; N1, n = 42; N2, n = 90; N3, n = 3) downloaded from the TCGA database were analyzed and presented as log2 normalized raw count (E). Data are shown as mean ± SEM from three independent experiments (ns, not significant; *, $p < 0.05$; **, $p < 0.01$; ***, $p < 0.001$).